

GAS: A Gaussian Mixture Distribution-Based Adaptive Sampling Method for PINNs

Yuling Jiao^{a,b}, Di Li^a, Xiliang Lu^{a,b}, Jerry Zhijian Yang^{a,b}, Cheng Yuan^{a,b}

^a*School of Mathematics and Statistics, Wuhan University, Wuhan, 430072, China*

^b*Hubei Key Laboratory of Computational Science, Wuhan University, Wuhan, 430072, China*

Abstract

With recent study of the deep learning in scientific computation, the PINNs method has drawn widespread attention for solving PDEs. Compared with traditional methods, PINNs can efficiently handle high-dimensional problems, while the accuracy is relatively low, especially for highly irregular problems. Inspired by the idea of adaptive finite element methods and incremental learning, we propose GAS, a Gaussian mixture distribution-based adaptive sampling method for PINNs. During the training procedure, GAS uses the current residual information to generate a Gaussian mixture distribution for the sampling of additional points, which are then trained together with history data to speed up the convergence of loss and achieve a higher accuracy. Several numerical simulations on 2d to 10d problems show that GAS is a promising method which achieves the state-of-the-art accuracy among deep solvers, while being comparable with traditional numerical solvers.

Keywords: Deep learning, adaptive sampling, PINN

2020 MSC: 68T07, 65N99

1. Introduction

In recent years, solving partial differential equations(PDEs) with deep learning methods has been widely studied, e.g., the Physics-Informed Neural Networks (PINNs) [1], the Deep Ritz Method (DRM) [2] and the Weak Adversarial Neural Networks (WAN) [3]. While Both DRM and WAN use the variational forms of the PDEs, PINNs solves PDEs by a direct minimization of the square residuals, which makes the method more flexible and easier to

be formulated to general problems. By reformulating the original PDE problems into a optimization problems, The physics-informed neural networks [1, 4, 5, 6] can easily approximate the solution of PDE with a deep neural network (DNN) function space, through minimizing the corresponding loss term which is defined as the integral of residuals. In practice, this integral is approximated by using Monte Carlo (MC) methods with finite points, which are usually sampled according to a uniform distribution on the computational domain. In contrast to classical computational methods, where the main concern is the approximation error, one needs to balance the approximation error and the generalization error for the neural network solvers, where the approximation error mainly originates from the modeling capability of the neural network, while the generalization error is mainly related to the discretization of loss with random samples. While a uniform random sampling strategy is simple to implement, the low regularity regions of the solution may not be taken consideration enough, which makes PINNs be inefficient and even inaccurate, especially when the problems is high dimensional.

To handel the singularity in solution, several sampling strategies have been developed to improve the efficiency and accuracy of PINNs. In [7], a simple residual-based adaptive refinement method RAR was proposed to iteratively add new points with the largest residuals in the training set. Later in [8], the authors give a comprehensive study of non-adaptive and residual-based adaptive sampling methods, with an extension of the RAR method to more general residual-based adaptive distribution methods (RAD and RAD-G), in which the added points are sampled from a combination of residual-induced density and uniform distribution. Meanwhile, by reformulating the loss functional with the idea of importance sampling [9, 10], the authors developed a KRnet-based method DAS to approximate the proposed density [11], which proves to be an effective way to capture the singularity of solution. More recently, inspired by the idea of adaptive finite element scheme, researchers studies a failure-informed adaptive sampling method FI-PINNs [12, 13], in which new points are added to better approximate the failure probability of PINNs. With the approximation of proposal density in the importance sampling of failure probability by Gaussians or Subset simulation, FI-PINNs shows a promising prospects in dealing with multi-peak and high dimensional problems.

In this paper, motivated by the concept of continual learning[14] and the key idea in adaptive FEM that one should refine meshes according to some posterior indicator[15], we proposed GAS, a Gaussian mixture distribution-

based adaptive sampling strategy as a region refinement method. Different from the DAS and FI-PINNs methods in which the adaptive sampling is aimed at the approximation of some proposed density in importance sampling, we define the distribution of added data by maximizing the risk with the new density. As a result, we select points where the residual is relatively bigger as means of Gaussians, and the gradient of residual at these points are used to construct the covariances respectively. After that, additional points sampled according to this mixture Gaussians will be added to the old training set, followed by the next training round of PINNs. With such an easy while effective incremental learning strategy, we successfully solved several highly irregular problems from 2 dimension to 10 dimension by PINNs, and our method achieve the state of the art in the field of adaptive sampling for PINNs.

The rest of this paper is organized as follows. In Section 2, a brief overview of PINNs will be presented. The GAS method is then constructed in section 3 and we demonstrate the efficiency of our method with numerical experiments in section 4. In Section 5 the main conclusion will be given.

2. Preliminaries of PINNs

Let $\Omega \in \mathbb{R}^d$ be a bounded spatial domain and $\mathbf{x} \in \mathbb{R}^d$. The PDE problem is stated as: find $u(\mathbf{x}) \in F : \mathbb{R}^d \mapsto R$ where F is a proper function space defined on Ω , such that:

$$\begin{cases} \mathcal{L}u(\mathbf{x}) = s(\mathbf{x}), & \forall \mathbf{x} \in \Omega, \\ \mathcal{B}u(\mathbf{x}) = g(\mathbf{x}), & \forall \mathbf{x} \in \partial\Omega. \end{cases} \quad (1)$$

Here \mathcal{L} and \mathcal{B} are operators defined in the domain and on the boundary respectively. Let $u(\mathbf{x}; \Theta)$ be a neural network with parameters Θ . In the framework of PINNs, the goal is to use $u(\mathbf{x}; \Theta)$ to approximate the solution $u(\mathbf{x})$ through optimizing the following loss function:

$$\begin{aligned} J(u(\mathbf{x}; \Theta)) &= \|r(\mathbf{x}; \Theta)\|_{2,\Omega}^2 + \gamma \|b(\mathbf{x}; \Theta)\|_{2,\partial\Omega}^2 \\ &= J_r(u(\mathbf{x}; \Theta)) + \gamma J_b(u(\mathbf{x}; \Theta)), \end{aligned} \quad (2)$$

where $r(\mathbf{x}; \Theta) = \mathcal{L}u(\mathbf{x}; \Theta) - s(\mathbf{x})$, $b(\mathbf{x}; \Theta) = \mathcal{B}u(\mathbf{x}; \Theta) - g(\mathbf{x})$, and $\gamma > 0$ is a penalty parameter. In practice, the loss functional (2) is usually discretized numerically by:

$$J_N(u(\mathbf{x}; \Theta)) = \|r(\mathbf{x}; \Theta)\|_{N_r, S_\Omega}^2 + \hat{\gamma} \|b(\mathbf{x}; \Theta)\|_{N_b, S_{\partial\Omega}}^2, \quad (3)$$

where $S_\Omega = \{\mathbf{x}_\Omega^{(i)}\}_{i=1}^{N_r}$ and $S_{\partial\Omega} = \{\mathbf{x}_{\partial\Omega}^{(i)}\}_{i=1}^{N_b}$ are two sets of uniformly distributed collocation points, and

$$\begin{aligned} \|u(\mathbf{x}; \Theta)\|_{N_r, S_\Omega} &= \left(\frac{1}{N_r} \sum_{i=1}^{N_r} u^2(\mathbf{x}_\Omega^{(i)}) \right)^{\frac{1}{2}}, \\ \|u(\mathbf{x}; \Theta)\|_{N_r, S_{\partial\Omega}} &= \left(\frac{1}{N_b} \sum_{i=1}^{N_b} u^2(\mathbf{x}_{\partial\Omega}^{(i)}) \right)^{\frac{1}{2}} \end{aligned}$$

are the empirical risks inside and on the boundary of Ω . Defining the following two minimizers

$$\begin{aligned} u(\mathbf{x}; \Theta^*) &= \arg \min_{\Theta} J(u(\mathbf{x}; \Theta)) \\ u(\mathbf{x}; \Theta_N^*) &= \arg \min_{\Theta} J_N(u(\mathbf{x}; \Theta)), \end{aligned} \quad (4)$$

we can decompose the error in PINNs as:

$$\begin{aligned} \mathbb{E}(\|u(\mathbf{x}; \Theta_N^*) - u(\mathbf{x})\|_\Omega) &\leq \mathbb{E}(\|u(\mathbf{x}; \Theta^*) - u(\mathbf{x})\|_\Omega) \\ &\quad + \mathbb{E}(\|u(\mathbf{x}; \Theta_N^*) - u(\mathbf{x}; \Theta^*)\|_\Omega). \end{aligned} \quad (5)$$

While the first term describes the approximation error related to the expressing capability of neural networks, the second term consists of the optimization error and the statistical error due to random sampling in the MC procedure. In this work, we focus on the reduction of statistical error by seeking for a better estimation of the true risk $J(u(\mathbf{x}; \Theta))$.

3. Our Method

For simplicity, we assume the boundary term in (3) has been well approximated and only consider $J_r(u(\mathbf{x}; \Theta))$, the loss inside Ω induced by the residual. Instead of solving the original problem (1) with a static pre-sampled dataset by PINNs, we adopt an incremental learning strategy to gradually capture the singularities in our problem.

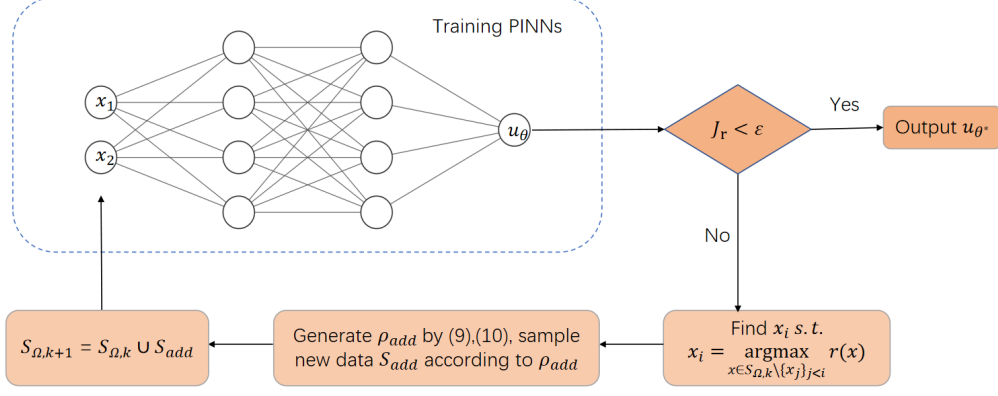


Figure 1: The flowchart of GAS method.

3.1. Active learning with risk maximization

To begin with, we first relax the definition of loss function J_r with a general background distribution $\rho(\mathbf{x})$ as follows:

$$J_r(u(\mathbf{x}; \Theta)) = \int r^2(\mathbf{x}; \Theta) \rho(\mathbf{x}) d\mathbf{x} \quad (6)$$

This relaxation, however, does not change the minimizer $u(\mathbf{x}; \Theta^*)$ if the minimal value is zero. In general, we may deliberately and actively select the background density $\rho(\mathbf{x})$ to focus on the learning of regions with higher risk, such as the neighbor of singularity. Similar with the least confident strategy in the literature of active learning [16], a naive searching method for $\rho(\mathbf{x})$ can be formulated as the problem of maximizing the present risk:

$$\Theta^*, \rho^*(x) = \arg \min_{\Theta} \max_{\rho(x) > 0, \int \rho(x) dx = 1} \int r^2(\mathbf{x}; \Theta) \rho(\mathbf{x}) d\mathbf{x} \quad (7)$$

However, without any constraints on the density function $\rho(\mathbf{x})$, the maximization problem in (7) leads to the following trivial solution:

$$\rho^*(\mathbf{x}) = \delta_{\mathbf{x}_0}(\mathbf{x}) \quad (8)$$

in which $r(\mathbf{x}, \Theta)$ achieves the maximum value at $\mathbf{x} = \mathbf{x}_0$, since we have

$$\begin{aligned} \int r^2(\mathbf{x}; \Theta) \rho(\mathbf{x}) d\mathbf{x} &\leq \max_{\mathbf{x}} r^2(\mathbf{x}; \Theta) \int \rho(\mathbf{x}) d\mathbf{x} \\ &\leq r^2(\mathbf{x}_0; \Theta). \end{aligned}$$

The singularity of the delta function $\delta_{\mathbf{x}_0}(\mathbf{x})$ makes it useless in practical since we only add new points at the maximal point of loss, given the current network parameter Θ . This pointwise correction would make the learning of $u^*(\mathbf{x}; \Theta)$ in PINNs rather inefficient. In the following, we would propose an incremental learning paradigm, in which the distribution of added points is restricted to some special function space for a more efficient sampling.

3.2. GAS: a Gaussian mixture distribution-based adaptive sampling method

Starting from the uniform distribution $\rho_0(\mathbf{x})$, we would sequentially trained PINNs and then adaptively sample and add new points according to some distribution, with which we can update the evaluation of loss and train the next round of PINNs. More specially, after k -round training of PINNs, we construct the following new distribution $\rho_{k+1}(\mathbf{x})$ as

$$\rho_{k+1}(\mathbf{x}; \eta) = \alpha_k \rho_{old}(\mathbf{x}) + (1 - \alpha_k) \rho_{add}(\mathbf{x}; \eta^k). \quad (9)$$

The first term $\rho_{old} \triangleq \rho_k$ in (9) stands for the data distribution used in previous training, with which we can review the learned knowledge and avoid the catastrophic forgetting phenomenon[17]. The second term is proposed to adaptively sample new points for a better description of the risk, with which we can localize the singularity and sample more points in high risk region. α_k is a hyperparameter introduced to balance the ratio of new knowledge and old knowledge.

Since the mixture of Gaussians is a simple and widely used distribution with the ability of modeling density with multi-peaks, we would use it to represent the distribution of added points:

$$\rho_{add}(\mathbf{x}; \eta^k) \triangleq \sum_{i=1}^{N_G} \pi_i^k \mathcal{N}(\mathbf{x} | \mu_i^k, \Sigma_i^k), \quad (10)$$

in which $\eta^k = \{\pi_i^k, \mu_i^k, \Sigma_i^k\}$ are tunable parameters and $\mathcal{N}(\mathbf{x} | \mu_i^k, \Sigma_i^k)$ is a Gaussian distribution with average μ_i^k and covariance Σ_i^k .

Following the spirit of adaptive finite element method, we use the residual function $r(\mathbf{x}; \Theta)$ as an indicator to determine the position of refined region. Taking the one-dimensional case as an example, the means and variance appeared in Gaussian can be determined by solving the following risk maximization problem:

$$\mu^*, \sigma^* = \arg \max_{\mu, \sigma} \int r^2(x; \Theta) \mathcal{N}(x|\mu, \sigma) dx \quad (11)$$

To derive an explicit expression for μ^* and σ^* , we would further simplify the calculation in (11) by using the idea of Laplace approximation [18]. Suppose $r(x; \Theta)$ has a unique local maximum point at $x = x_0$, by writing $r(x; \Theta)$ as

$$r(x; \Theta) = e^{-V(x)} \quad (12)$$

and taking the second order Taylor's expansion of $V(x)$ at x_0 , we have

$$r(x; \Theta) = e^{-[V(x_0) + V'(x_0)(x-x_0) + \frac{1}{2}V''(x_0)(x-x_0)^2]} \quad (13)$$

$$= C \cdot e^{-\frac{1}{2}V''(x_0)(x-x_0)^2} \quad (14)$$

Here C is constant independent of x and we have used the fact $V'(x_0) = 0$ since x_0 is a maximum point. Denote $V''(x_0) = \frac{1}{2a^2}$ and Substitute (14) into (11), we have

$$\mu^*, \sigma^* = \arg \max_{\mu, \sigma} \int r^2(x; \Theta) \mathcal{N}(x|\mu, \sigma) dx \quad (15)$$

$$= \arg \max_{\mu, \sigma} \frac{C^2}{\sqrt{2\pi}\sigma} \int e^{-[V''(x_0)(x-x_0)^2 + \frac{(x-\mu)^2}{2\sigma^2}]} dx \quad (16)$$

$$= \arg \max_{\mu, \sigma} \frac{1}{\sigma} \int e^{-[\frac{(x-x_0)^2}{2a^2} + \frac{(x-\mu)^2}{2\sigma^2}]} dx \quad (17)$$

$$= \arg \max_{\mu, \sigma} \frac{1}{\sigma} \int e^{-[(\frac{1}{2\sigma^2} + \frac{1}{2a^2})(x - \frac{a^2\mu + \sigma^2 x_0}{a^2 + \sigma^2})^2 + \frac{(\mu - x_0)^2}{2a^2 + 2\sigma^2}]} dx \quad (18)$$

$$= \arg \max_{\mu, \sigma} \frac{e^{-\frac{(\mu - x_0)^2}{2a^2 + 2\sigma^2}}}{\sigma} \int e^{-[(\frac{1}{2\sigma^2} + \frac{1}{2a^2})(x - \frac{a^2\mu + \sigma^2 x_0}{a^2 + \sigma^2})^2]} dx \quad (19)$$

$$= \arg \max_{\mu, \sigma} \frac{1}{\sigma} \sqrt{\frac{2\sigma^2 a^2}{\sigma^2 + a^2}} \cdot e^{-\frac{(\mu - x_0)^2}{2a^2 + 2\sigma^2}} \quad (20)$$

$$= \arg \max_{\mu, \sigma} \sqrt{\frac{2}{1 + (\sigma/a)^2}} \cdot e^{-\frac{(\mu - x_0)^2}{2a^2 + 2\sigma^2}} \quad (21)$$

As mentioned in the end of last subsection 3.1, without any constraint of the covariance σ , the best proposal density ρ_{add} will collapse to the delta function $\delta_{x_0}(x)$. This can be seen from the last term in (21), which can only take the maximum when $\sigma = 0$. To avoid this, we restrict the covariance to that $\sigma \geq a$. In this case, the maximum value in (11) can be obtained at

$$\mu = x_0, \quad \sigma = a = [2V''(x_0)]^{-1/2} \quad (22)$$

According to (12) and the fact that $r'(x_0) = 0$, $V''(x_0)$ can be calculated as

$$V''(x_0) = -\frac{r''(x_0)}{r(x_0)} \quad (23)$$

On the other hand, since a second order derivative of r may require two times back propagation in the network computation, which would make the searching of ρ_{add} inefficient, we would replace the $r''(x_0)$ with its difference approximation:

$$V''(x_0) \approx -\frac{r'(x_0 + \epsilon)}{\epsilon \cdot r(x_0)} \quad (24)$$

In practice, the maximum point x_0 of $r(x)$ can be approximated by the sample \hat{x}_0 , which is the maximum point of $r(x)$ obtained in a finite dataset, e.g., all the sample data used in the k-round training of PINNs. In this case, we may hope the difference $|x_0 - \hat{x}_0| = O(\epsilon)$, and compute the variance σ as

$$\sigma = [2V''(x_0)]^{-1/2} = \left| \frac{r(\hat{x}_0)}{2} \epsilon \right|^{1/2} \cdot |r'(\hat{x}_0)|^{-1/2}. \quad (25)$$

A formal understanding of the selection in (22)(25) is that, we hope to sample additional data around the points with highest risk, and a more rapidly decrease of the local risk indicates less points should be sampled far away from the means.

In high dimensional case, we may similarly generate the proposed density ρ_{add} as mixture of Gaussians, with the means and variances defined as follows:

$$\mu_i^k = \arg \max_{x \in S_{\Omega,k}} r(\mathbf{x}; \Theta), \quad (26)$$

$$\Sigma_i^k = \lambda [\text{diag}(\nabla_x r(\mathbf{x}; \Theta)|_{x=\mu_i^k})]^{-1}. \quad (27)$$

Here $S_{\Omega,k}$ is the dataset used in the k-round training of PINN, λ is a hyper-parameter and $\text{diag}(\alpha)$ refers to diagonal matrix with the diagonal element

vector being α . In the following numerical examples, we will use the top N_G points with largest residual, instead of using the N_G local maximum point of $r(x)$ to calculate the means. This compromise, however, has little influence on the effectiveness of our method, as long as N_G is not too small. With the new distribution $\rho_{k+1} = \alpha_k \rho_k + (1 - \alpha_k) \rho_{add}$, the evaluation of J_r can be updated as

$$J_r^{k+1}(u(\mathbf{x}; \Theta)) = \int r^2(\mathbf{x}; \Theta) \rho_{k+1}(\mathbf{x}) d\mathbf{x}. \quad (28)$$

Then we may repeat the training process of PINNs by minimizing J_r^{k+1} . The flowchart of our method is shown in Figure 1.

A detail description of our idea is presented in Algorithm 1. As shown in the next section, this simple adaptive sampling strategy supply us with an effective and easy-to-implement method for solving elliptic equations with singularity, in both low dimension and high dimension case.

4. Numerical experiments

4.1. One-peak problem

Example 4.1. As a benchmark test, we first consider the following elliptic problem

$$\begin{cases} -\Delta u(x_1, x_2) &= s(x_1, x_2), \text{ in } \Omega, \\ u(x_1, x_2) &= g(x_1, x_2), \text{ on } \partial\Omega, \end{cases} \quad (29)$$

where $\Omega = [-1, 1]^2$. The reference solution is chosen as follows:

$$u(x_1, x_2) = \exp(-1000[(x_1 - r_c)^2 + (x_2 - r_c)^2]),$$

which has a peak at the point (r_c, r_c) and decreases rapidly away from (r_c, r_c) .

Due to the highly singularity at the peak point, a uniform distribution-based loss would make the PINNs rather inefficient. In this example, we choose a six-layer fully connected neural network $u(\mathbf{x}; \Theta)$ with 32 neurons to approximate the solution, and uniformly sample $N_r = 500$ points in Ω and $N_b = 200$ points on the boundary. During the incremental learning, we train $N_p = 3000$ epochs for PINNs after each adaptive sampling and the number of adaptive sampling times is set as $N_a = 10$. The batch size m is chosen as 500 for the points in S_Ω and 200 for boundary samples.

Algorithm 1 GAS

Input: $u(\mathbf{x}; \Theta^{(0)})$, maximum epoch number for PINNs N_p , number of times for adaptive sampling N_a , number of Gaussians in the mixture distribution N_G , batch size m , positive parameters λ , initial training set $S_{\Omega,0} = \{\mathbf{x}_{\Omega,0}^{(i)}\}_{i=1}^{N_r}$ and $S_{\partial\Omega,0} = \{\mathbf{x}_{\partial\Omega,0}^{(i)}\}_{i=1}^{N_b}$, validated set $S_{valid} = \{\mathbf{y}^{(i)}\}_{i=1}^{N_t}$

Output: $u(\mathbf{x}; \Theta_N^*)$

while $k \leq N_a - 1$ and $J_r \leq \epsilon$ **do**

for $i = 0$ **to** $N_p - 1$ **do**

for j **steps do**

 Sample m samples from $S_{\Omega,k}$.

 Sample m samples from $S_{\partial\Omega,k}$.

 Update $u(\mathbf{x}; \Theta)$ by SGD of $J_N(u(\mathbf{x}; \Theta))$.

end for

end for

 Calculate all residuals in $\{\mathbf{y}^{(i)}\}_{i=1}^{N_t}$ by (3).

 Sort the validated points according to the residuals in a descending order to obtain $\tilde{y}^{(1)}, \tilde{y}^{(2)}, \dots, \tilde{y}^{(N_t)}$

for $t = 0$ **to** $N_G - 1$ **do**

 Construct a Gaussian distribution $\mathcal{N}^{(t)}(\mu, \Sigma)$ by the coordinates of $\tilde{y}^{(t)}$ as the mean μ and the gradient of residual to its coordinates as the reciprocal of the covariance Σ .

 Generate one or more points, denoted as the set $S_g^{(t)}$, which are sampled from $\mathcal{N}^{(t)}(\mu, \Sigma)$.

end for

 Add all the points so that $S_{\Omega,k+1} = S_{\Omega,k} \cup S_g^{(0)} \cup S_g^{(1)} \dots \cup S_g^{(N_G-1)}$

 Add points in boundary from uniform distribution so that the ratio of the points in $S_{\Omega,k}$ to the points in $S_{\partial\Omega,k}$ is a constant.

end while

Table 1: MSE for different methods and point sets in one-peak problem.

MSE \ $ S_\Omega $	2000	3000	4000	5000
Strategy				
Uniform	7.5E-03	7E-03	3E-03	1E-03
DAS	4E-03	8E-04	7.5E-04	4E-04
GAS	4.9E-04	2.2E-04	1.8E-04	2.9E-05

As for parameters in GAS, we set $N_G = 20$ to construct the Gaussian mixture model and sample 25 points from each Gaussian, thus a total of 500 points would be added into S_Ω during each adaptive sampling. To maintain the ratio of interior and boundary points, we add 200 points additionally into $S_{\partial\Omega}$, which are simply sampled by uniform distribution.

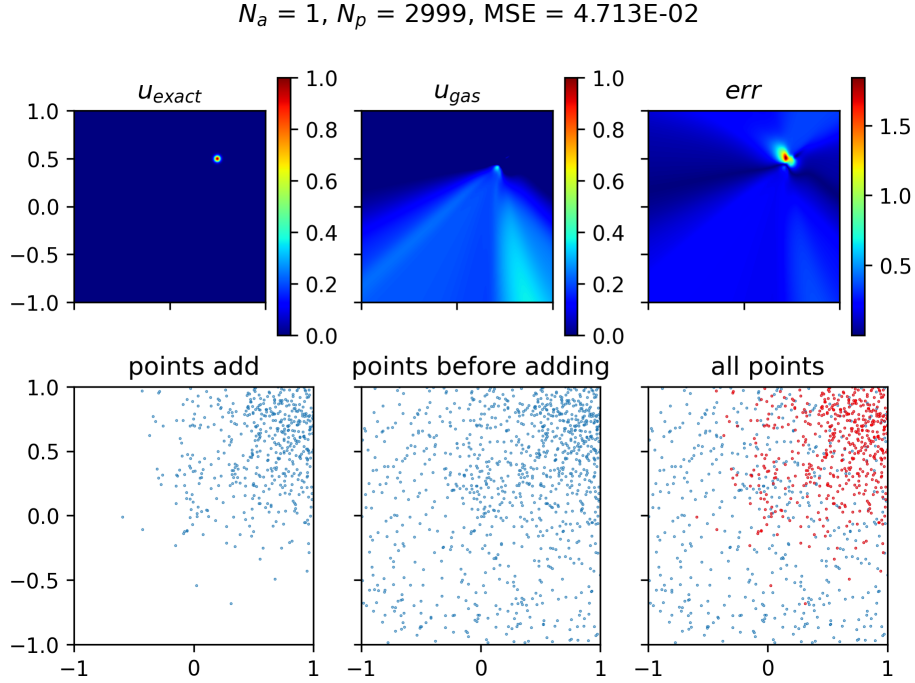


Figure 2: PINNs with 1st mesh points in one peak problem and now $|S_\Omega| = 1000$.

Figure 2, 3, 4 shows the numerical result of PINNs after 1 time, 5 times and 9 times of adaptive sampling. According to these, we can see that the magnitude of error becomes smaller with the times of adaptive sampling increasing. The solution by GAS converges almost to the exact solution after 3000 samples have been used, while the PINNs method with a uniform sampling strategy fails to deal with the point singularity (see Figure 5). Since the solution owns one peak at $(0.5, 0.5)$, the aggregated additional samples are mainly located around this singular point where the residual is much bigger, which is exactly we expect. A further comparison of our method with the results by using uniform sampling and DAS method is shown in Table 1,

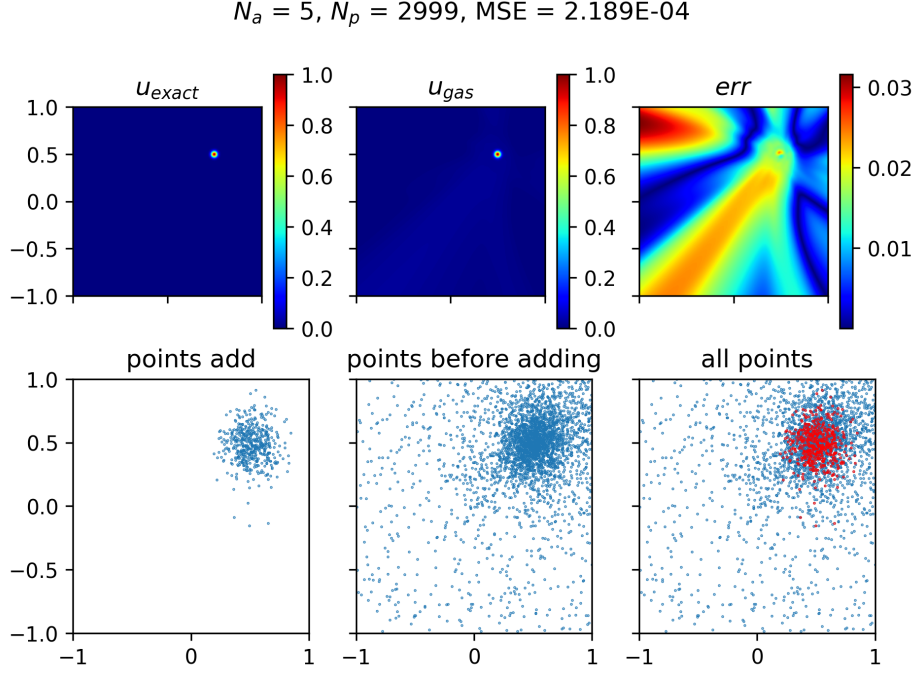


Figure 3: PINNs with 5-th adaptive mesh point in one peak problem and now $|S_\Omega| = 3000$.

which reveals that our method can achieve a uniformly better mean-square error (MSE), given a fixed sampling size of S_Ω . Specially, the MSE by GAS may achieve $O(10^{-5})$, which is better than the $O(10^{-4})$ by DAS and $O(10^{-3})$ with uniform distribution.

4.2. two-peaks problem

Example 4.2. Next we consider the following elliptic equation with two peaks:

$$\begin{cases} -\nabla \cdot [u(x_1, x_2) \nabla (x_1^2 + x_2^2)] + \Delta u(x_1, x_2) = s(x_1, x_2), & \text{in } \Omega, \\ u(x_1, x_2) = g(x_1, x_2), & \text{on } \partial\Omega, \end{cases} \quad (30)$$

where $\Omega = [-1, 1]^2$. The reference solution is set as

$$\begin{aligned} u(x_1, x_2) = & \exp(-1000[(x_1 - 0.5)^2 + (x_2 - 0.5)^2]) \\ & + \exp(-1000[(x_1 + 0.5)^2 + (x_2 + 0.5)^2]), \end{aligned}$$

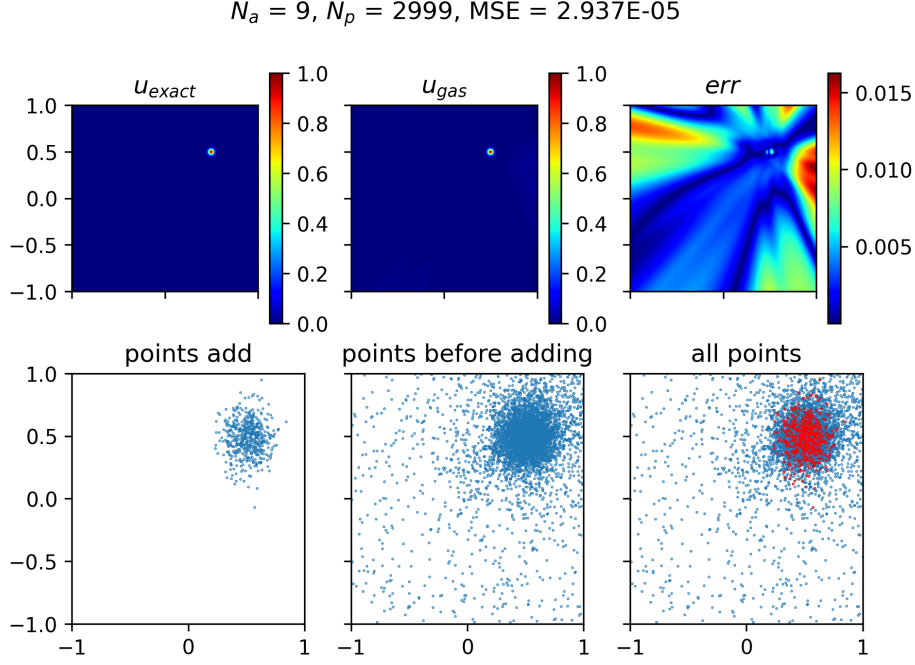


Figure 4: PINNs with 9-th adaptive mesh point in one peak problem and now $|S_\Omega| = 5000$.

which has two peaks at the points $(0.5, 0.5)$ and $(-0.5, -0.5)$.

In this example, we also set the initial size of dataset as $N_r = 500$ and $N_b = 200$, which are sampled from uniform distribution. The other parameters are selected as $N_p = 5000$, $N_a = 20$ and the batch size m for points in S_Ω and $S_{\partial\Omega}$ are set as 500 and 200. The hyperparameters for Gaussian mixture distributions are kept as in previous example.

As shown in Figure 6, 7, 8, 9, the GAS method does help us to find the singularity region during the training of PINNs, while a uniform distribution-based loss can hardly be convergent. This can be understood that with more points around the two peaks in solution are sampled and added into the training dataset (see the second row of each figure), the finetuned loss functional may better represent the real risk of the approximation by PINNs. Another fact worthy to be noticed is that the additional data is added alternately between different peaks in the early stage of learning, which is due to the active learning strategy defined by (26). This phenomenon, however, does

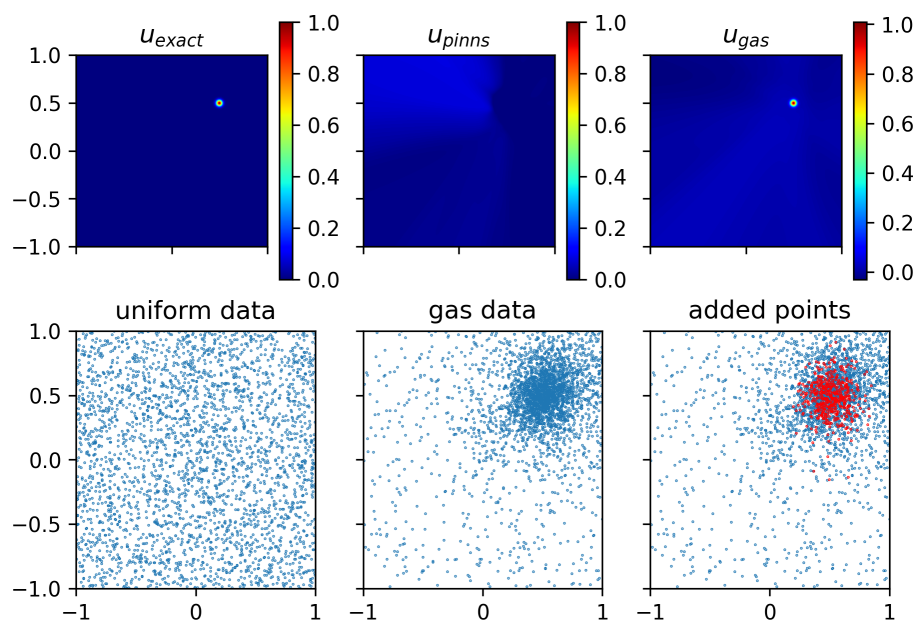


Figure 5: Solutions and 3000 points for uniform and GAS

Table 2: MSE for different methods and point sets in two-peak problem.

MSE \ $ S_\Omega $	2500	5000	7500	10000
Strategy				
Uniform	7.5E-02	1.7E-01	8E-02	3E-02
DAS	2E-02	7E-03	4.5E-03	1.5E-03
GAS	6.5E-03	5.6E-04	1.7E-04	4.1E-05

not break the convergence of GAS with the adaptive sampling continuing, and it can be avoided by using a set of local minimizers of $r(\mathbf{x}; \Theta)$ as means of Gaussians. We will leave this detail as future study.

In Table 2, we also present the MSE along with different training size by GAS, DAS and uniform sampling strategy. As before, the GAS method always achieves best accuracy among these methods, and the error of GAS is one order smaller than DAS.

4.3. High-dimensional linear problem

Example 4.3. As the third example, we would validate the efficiency of GAS in high dimensional case by studying the following d -dimensional problem:

$$-\Delta u(\mathbf{x}) = s(\mathbf{x}), \mathbf{x} \in \Omega. \quad (31)$$

where $\Omega = [-1, 1]^d$. We use the following reference solution

$$u(\mathbf{x}) = e^{-10\|\mathbf{x}\|_2^2}.$$

with Dirichlet boundary condition on $\partial\Omega$.

In this example, we focus on the case with $d = 10$. A six-layer fully connected neural network $u(\mathbf{x}; \Theta)$ with 64 neurons would be used to approximate the solution, and the size of initial dataset are set as $N_r = 10000$ and $N_b = 10000$, which are sampled from uniform distribution. We let $N_p = 3000$, $N_a = 20$ and the batch size $m = 5000$ for the points in S_Ω and $S_{\partial\Omega}$. To measure the quality of approximation, a tensor grid with n_t^d points are generated around the origin(in $[-0.1, 0.1]^d$) where $n_t = 3$ is the number of nodes in each dimension. With these grid points, we can calculate the following relative error by using numerical integration:

$$\text{Relative error} = \frac{\|u_\Theta - u_{exact}\|_2}{\|u_{exact}\|_2}.$$

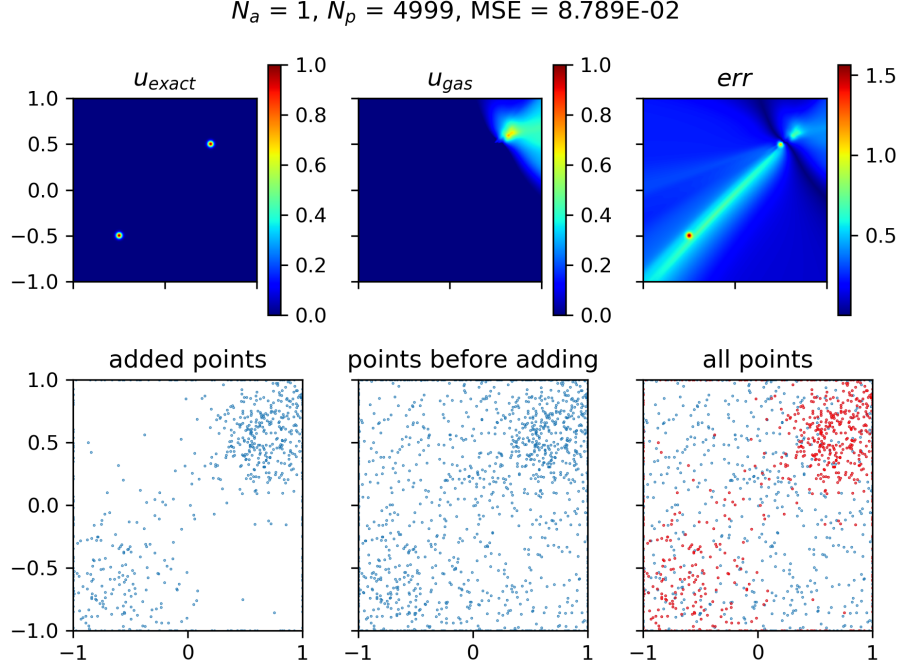


Figure 6: PINNs with 1st mesh points in two peak problem and $|S_\Omega| = 1000$.

Here u_Θ and u_{exact} denote the discrete vector of the numerical solution and exact solution.

In order to be comparable with the dataset used in [11], the number of Gaussians in the mixture model is set as $N_G = 40$ and we sample 250 points from each Gaussian distribution, which supply us with 10000 points at each time of adaptive sampling. For a better description of the size of data and cost of training, we denote the final number of different samples used by GAS as FNS, and the accumulated number of samples involved in the incremental learning as ANS. With N_a times adaptive sampling and $|S_\Omega|$ samples added in each time, the ANS and FNS can be calculated as

$$\begin{aligned} FNS &= N_a \times |S_\Omega| \\ ANS &= \frac{FNS}{N_a} \sum_{i=1}^{N_a} i, \end{aligned}$$

and the total computational cost of GAS can be defined as $ANS \times N_p$.

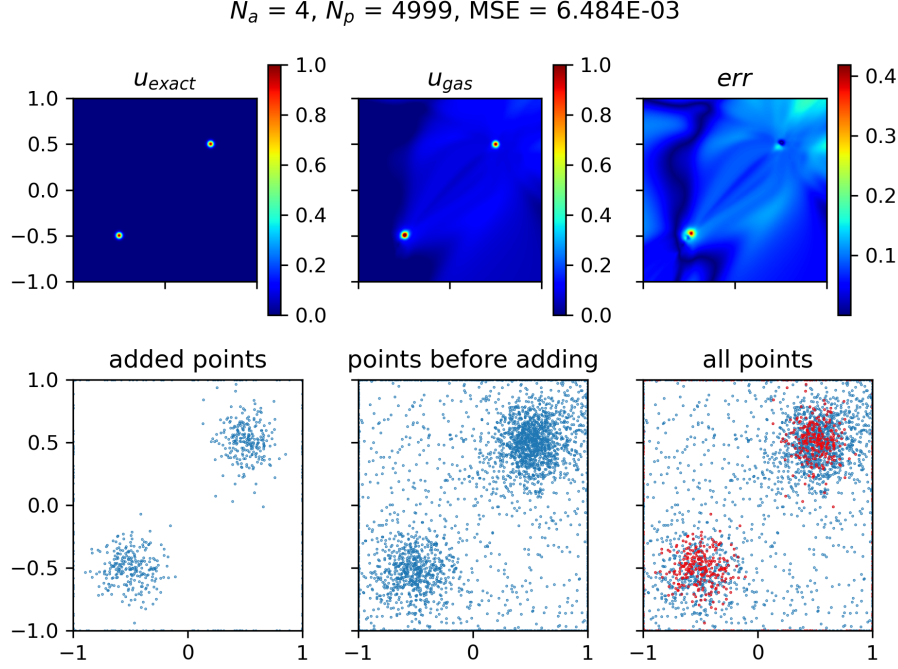


Figure 7: PINNs with 4-th adaptive mesh point in two peak problem and $|S_\Omega| = 2500$.

Since the DAS-G sampling strategy takes less time and achieves smaller errors than RAR, Uniform and DAS-R (see Table 1 in [11]), we would only compare the error and cost between GAS and DAS-G. As shown in Table 3, our method can achieve a smaller error even with less FNS and ANS, e.g., the error of GAS trained with 5.5×10^5 points sampled from 1×10^5 different samples is 5×10^{-1} , which is smaller than 8×10^{-3} , the error of DAS with 6×10^5 points sampled from 2×10^5 different samples. In general, our method can achieve better accuracy by using less data and computational cost, without mention to the fact that an additional KRnet needed in DAS may further increase the training time.

To further demonstrate the efficiency of GAS for high dimensional problems, we also plot the relative L_2 error of GAS with increasing dataset, and compare it with the FIPINNs method. As shown in Figure 10 and the Figure 12 in [12], with the $|S_\Omega|$ increasing, the error by GAS decrease faster than that by FIPINNs, which indicates that our method may better alleviates the

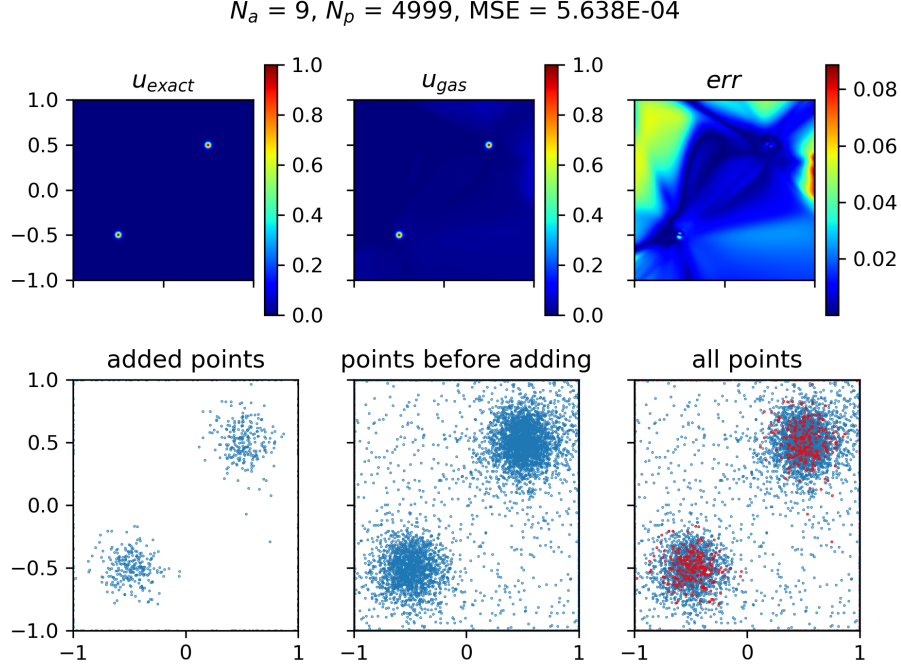


Figure 8: PINNs with 9-th adaptive mesh point in two peak problem and $|S_\Omega| = 5000$.

curse of dimensionality.

To visualize the adaptive training process in GAS, the loss and L_2 error with different N_G are also depicted in Figure 11. As we can see, the L_2 error converges to $O(1 \times 10^{-5})$ after 5 times of adaptive sampling. Before the first time GAS, the loss would converges to a rather small level while the L_2 error is almost unchanged, this reflects that the training of PINNs with a uniform distributed dataset would be misled to a trivial false solution, since statistically the points around singularity is rarely sampled. The following periodic jump in loss stands for the adjustment of risk introduced by the newly added points in GAS. Numerically, once the number of Gaussians in the mixture model reaches some value ($N_G = 20$ in this case), the increasing of N_G would bring little gains in the L_2 error.

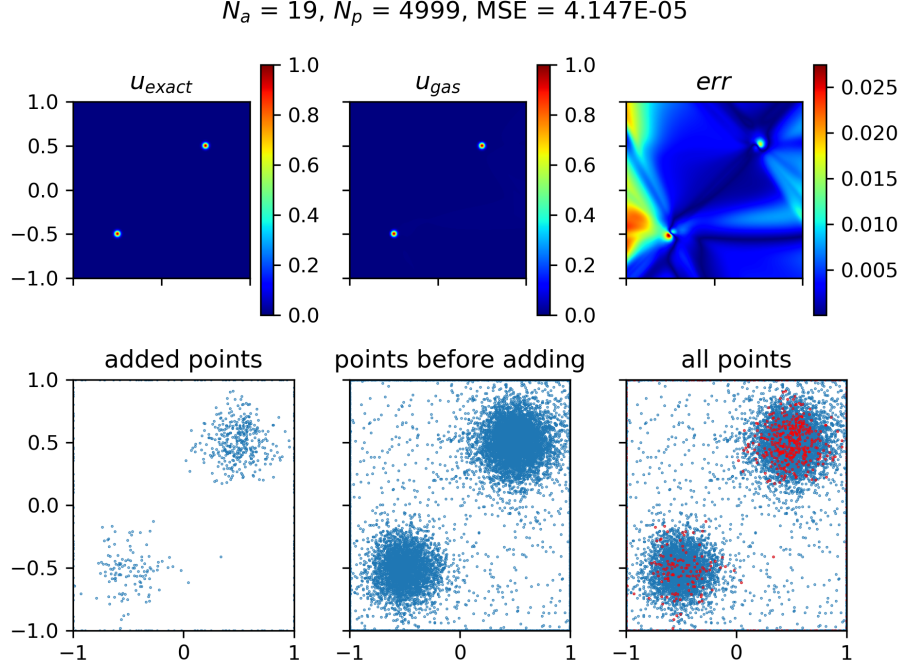


Figure 9: PINNs with 19-th adaptive mesh point in two peak problem and $|S_\Omega| = 10000$.

5. Conclusion

In this paper we have developed a Gaussian mixture distribution-based adaptive sampling (GAS) method and apply it into the training of physics-informed neural networks. The key idea of GAS is to construct a Gaussian mixture model to generalize additional and important knowledge during the incremental learning. By using the coordinates and gradients of points with larger residual to define the means and covariances, our method may actively localize the singular region of the solution and speed up the convergence of PINNs method. Compared to existing adaptive nonuniform sampling methods, GAS is easier to be implemented and may achieve lower error with even less training data and computational cost. Nevertheless, a systematically and rigorous analysis may better help us understand the efficiency and restriction of GAS, and the extension of GAS to more complex problems (e.g., use a deep generative model to replace the mixture model or use GAS to deal with problems with defects beyond point singularity), may further increase the

Table 3: errors for different methods in ten-dimensional linear test problem.

(error, ANS) \ strategy	DAS	GAS
FNS		
5×10^4	(0.030, 1.5×10^5)	(0.014, 1.5×10^5)
1×10^5	(0.028, 3×10^5)	(0.005, 5.5×10^5)
2×10^5	(0.008, 6×10^5)	(0.001, 2.1×10^6)

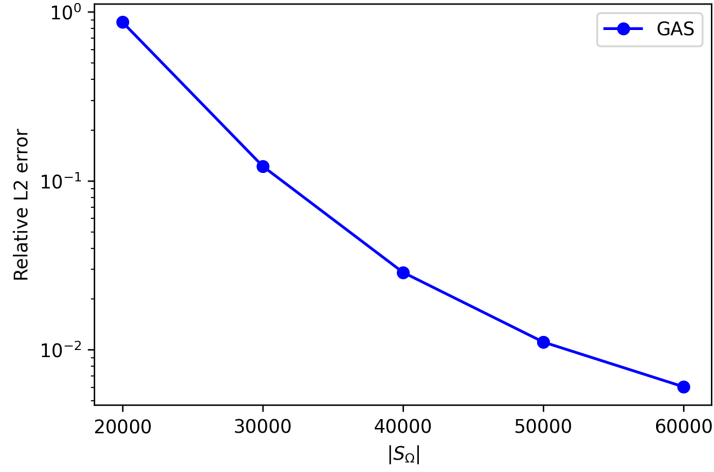


Figure 10: Relative L2 errors for ten dimension.

power of PINNs in solving high dimensional singular problems. We would leave these topics as out future study.

References

- [1] M. Raissi, P. Perdikaris, G. E. Karniadakis, Physics-informed neural networks: A deep learning framework for solving forward and inverse problems involving nonlinear partial differential equations, *Journal of Computational physics* 378 (2019) 686–707.
- [2] E. Weinan, B. Yu, The deep ritz method: A deep learning-based numerical algorithm for solving variational problems, *Communications in Mathematics and Statistics* 6 (2018) 1–12.

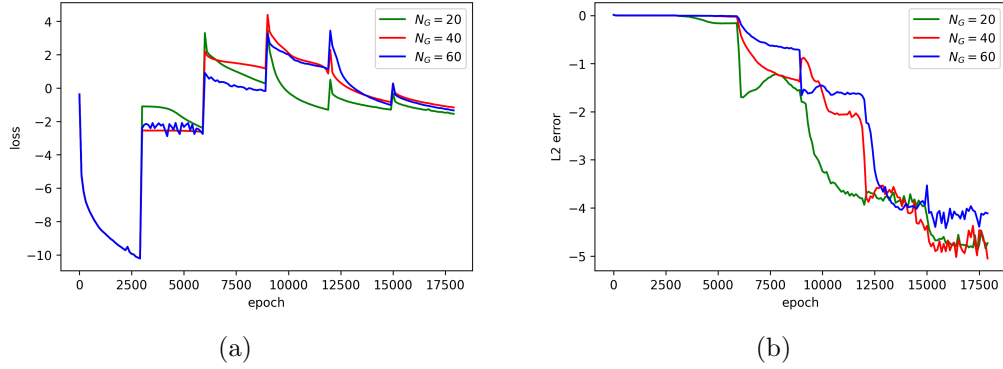


Figure 11: The loss (a) and relative L_2 error (b) of GAS for different N_G in ten dimension case.

- [3] Y. Zang, G. Bao, X. Ye, H. Zhou, Weak adversarial networks for high-dimensional partial differential equations, *Journal of Computational Physics* 411 (2020) 109409.
- [4] G. E. Karniadakis, I. G. Kevrekidis, L. Lu, P. Perdikaris, S. Wang, L. Yang, Physics-informed machine learning, *Nature Reviews Physics* 3 (2021) 422–440.
- [5] J. Sirignano, K. Spiliopoulos, Dgm: A deep learning algorithm for solving partial differential equations, *Journal of computational physics* 375 (2018) 1339–1364.
- [6] G. Pang, L. Lu, G. E. Karniadakis, fpinns: Fractional physics-informed neural networks, *SIAM Journal on Scientific Computing* 41 (2019) A2603–A2626.
- [7] L. Lu, X. Meng, Z. Mao, G. E. Karniadakis, Deepxde: A deep learning library for solving differential equations, *SIAM review* 63 (2021) 208–228.
- [8] C. Wu, M. Zhu, Q. Tan, Y. Kartha, L. Lu, A comprehensive study of non-adaptive and residual-based adaptive sampling for physics-informed neural networks, *Computer Methods in Applied Mechanics and Engineering* 403 (2023) 115671.

- [9] A. Katharopoulos, F. Fleuret, Not all samples are created equal: Deep learning with importance sampling, in: International conference on machine learning, PMLR, 2018, pp. 2525–2534.
- [10] M. A. Nabian, R. J. Gladstone, H. Meidani, Efficient training of physics-informed neural networks via importance sampling, *Computer-Aided Civil and Infrastructure Engineering* 36 (2021) 962–977.
- [11] K. Tang, X. Wan, C. Yang, Das-pinns: A deep adaptive sampling method for solving high-dimensional partial differential equations, *arXiv preprint arXiv:2112.14038* (2021).
- [12] Z. Gao, L. Yan, T. Zhou, Failure-informed adaptive sampling for pinns, *arXiv preprint arXiv:2210.00279* (2022).
- [13] Z. Gao, T. Tang, L. Yan, T. Zhou, Failure-informed adaptive sampling for pinns, part ii: combining with re-sampling and subset simulation, *arXiv preprint arXiv:2302.01529* (2023).
- [14] R. Hadsell, D. Rao, A. A. Rusu, R. Pascanu, Embracing change: Continual learning in deep neural networks, *Trends in cognitive sciences* 24 (2020) 1028–1040.
- [15] R. H. Nochetto, K. G. Siebert, A. Veiser, Theory of adaptive finite element methods: an introduction, in: Multiscale, nonlinear and adaptive approximation, Springer, 2009, pp. 409–542.
- [16] B. Settles, *Active learning literature survey* (2009).
- [17] R. M. French, Catastrophic forgetting in connectionist networks, *Trends in cognitive sciences* 3 (1999) 128–135.
- [18] C. M. Bishop, N. M. Nasrabadi, *Pattern recognition and machine learning*, volume 4, Springer, 2006.